SSRG International Journal of Electronics and Communication Engineering
ISSN: 2348-8549/ https://doi.org/10.14445/23488549/IJECE-V10I12P109

Volume 10 Issue 12, 93-101, December 2023

Original Article

Design of Multiband Diamond Fern Fractal Microstrip Patch Antenna for Vehicular Application Systems

N. Porchelvi[1], S. Titus[2]

[1]*Department of ECE, Vivekanandha College of Technology for Women, Tamilnadu, India.*
[2]*Department of EEE, K. Ramakrishnan College of Engineering, Tamilnadu, India.*

[1]*Corresponding Author : nporchelviresearchscholar@gmail.com*

Received: 11 October 2023 Revised: 22 November 2023 Accepted: 13 December 2023 Published: 23 December 2023

Abstract *- This investigation aims to build a brand-new Diamond Fern Fractal Antenna (DFFA) with a microstrip patch line to be utilised in car application systems. The suggested antenna is distinct from previous examples in that its patch is oriented in a manner that is intended to maximise bandwidth while simultaneously lowering return loss. The slots are inserted into the diamond patch, manufactured in this design based on an inexpensive FR-4 glass epoxy substrate with a relative permittivity of 4.4 and an overall dimension of 25 by 25 by 1.6 mm^3. In addition, it assists in the enhancement of the multiband features as well as the bandwidth, and its efficacy is tested with the assistance of design equations and HFSS simulation software. In addition, the technique for the parameter extraction of the suggested DFFA design is thoroughly explained in this paper. Compared with other methods, the DFFA constructed with 16 slots offers superior performance in improved bandwidth, impedance matching, frequency bands, and Gain.*

Keywords *- Global System for Mobile (GSM), Diamond Fern Fractal Antenna (DFFA), Microstrip patch, Multiband characteristics, Bandwidth, Return loss, Wireless Local Area Networks (WLAN).*

1. Introduction

Recently, there has been an increased demand for wireless systems and devices due to the rapid development of internet and communication technology. Among others, the low-profile systems significantly gained more attraction from many researchers for enhancing vehicular communication. Conventional communication systems highly require small-size broadband antennas and are also straightforward to design and implement.

Hence, different miniaturisation techniques are developed for creating small compact antennas, where the substrate is used with a high dielectric constant. Moreover, the miniaturised antennas are designed with improved electrical length by applying different impedance loads [1-3]. The fractal is one of the most popular and extensively used antenna design techniques, which helps model small antennas with high resonant frequency and gain efficiency. Due to their suitability, fractal geometries are increasingly used in antenna design, and they have recently acquired a significant attraction for developing compact personal components. Specifically, the space-filling property of fractal geometry helps minimise the antenna size, and its self-similarity property could be more helpful in designing multiband fractal antennas [4-7]. In other words, it is defined as the fractal antenna that uses the fractal geometry to maximise the material length to transmit or receive the signals within a surface area.

Hence, fractal antennas are compact and enormously used in many telephonic and microwave communication systems. Compared to the other antenna models, it can optimally operate under varying frequencies [8-12]. Conventionally, the different types of antennas such as Slot, travelling wave, microstrip, YagiUda, patch and fractal are developed for an enormous application system such as:

- Bluetooth
- WiFi
- WiMax
- WLAN
- High-speed point-point communication systems
- Infrared, satellite and mobile communication
- Networking applications like MANET, VANET, GPRS, etc.

Moreover, the design and development of antennas used for separate wireless application/communication systems are currently tedious and challenging tasks. Because improving the performance parameters like bandwidth, resonant

frequency, gain, etc., is a highly essential process that needs to be accomplished in the antenna design. Among other types, the microstrip and fractal antennas provide better performance outcomes due to their compact size, signal output, multi-frequency operation, linear and circular polarisation, easy deployment, and economical production. This paper proposes to model a new Diamond Fern Fractal Antenna (DFFA) for vehicular communication systems. The main objective of this research work is to model a compact and efficient DFFA with increased bandwidth, resonant frequency, and gain efficiency [13-17]. Furthermore, a novel method has been deployed to obtain multiband characteristics and perfect impedance matching in a compact antenna.

2. Proposed Method

The Diamond Fern Fractal Antenna (DFFA) that has been proposed has the top of the substrate and a partial ground plane on the rear side. The diamond patch is made by designing a square patch with dimensions of 25mm in length and breadth, then tilting the square patch to the right by 45 degrees. Figure 1 and Figure 2 demonstrate, respectively, the design phases that were iterated multiple times, as well as the final geometry of the presented DFFA. In this configuration, the patch antenna begins with four rectangular slots in the first iteration, and the number of slots after that rises with each subsequent iteration. The antenna's bandwidth efficiency can be improved by utilising these cutting slots in strategic locations. In addition, the partial ground is modelled with a length of 6mm and a width of 25mm, respectively, which improves the return loss characteristics. After the feedline has been built to provide good impedance matching with the input port, the antenna is loaded with sixteen slots with a width of 0.5 millimetres that are symmetrically distributed on both sides.

In addition, it is fed by a microstrip line feed, which is one of the most effective methods for fabricating the antenna. It is also easy to model and straightforward to match with the inset location [18-20]. FR4, which has a relative permittivity of 4.4, is used in the design of the printed antenna, and the thickness of the substrate is 1.6 millimetres. The suggested DFFA has dimensions of 25 millimetres on a side and 1.6 millimetres on a side, with the length L and width W of the antenna being determined by applying the following model:

$$L = W = \frac{\lambda}{2}\sqrt{\frac{2}{Er+1}}mm \quad (1)$$

The antenna design parameters and their dimensions are represented in Table 1, and the final fabricated antenna is shown in Figure 3.

Fig. 1 Shows the design steps of the proposed antenna model

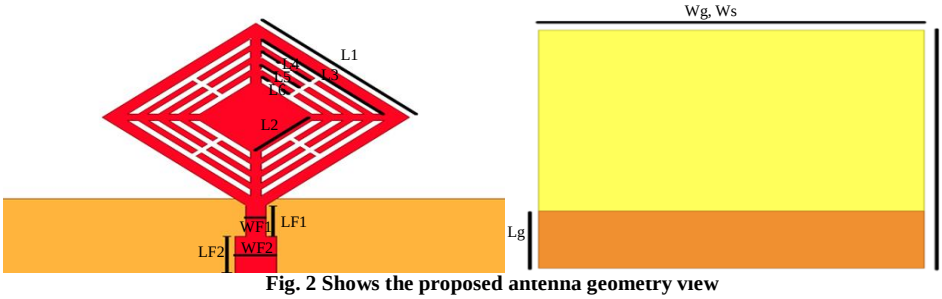

Fig. 2 Shows the proposed antenna geometry view

Table 1. Designing parameters of the proposed DFFA

Parameter	Dimension (mm)
LFI	3
WF1	1
LF2	3
WF2	2
LG	6
WG	25
LS	25
WS	25

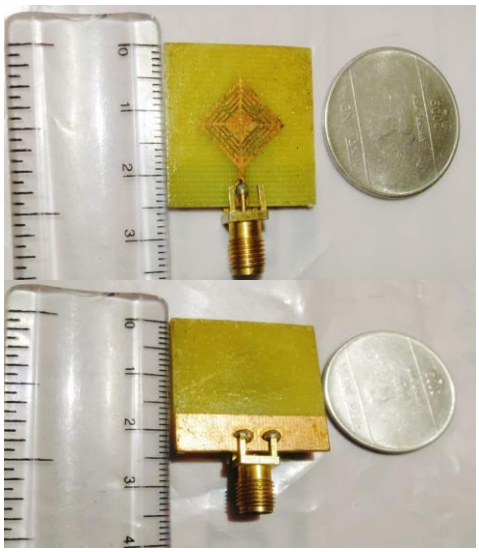

Fig. 3 The fabric of the proposed antenna (top and bottom view)

The proposed antenna's return loss and resonant frequency are assessed with the length and width of each slot in Table 2. The DFFA includes the slots from L1 to L9, each having separate length and width dimensions. Then, the resonant frequency is distinctly estimated for each slot with its return loss characteristics.

Typically, the length of the resonant antenna is effectively determined based on the underlying principles of frequency reconfiguration. The return loss is the parameter mainly used to estimate the loss of power in the signal in terms of dB, which must be reduced by adequately designing the antenna. According to the analysis, it is observed that the L1 slot, which has a length and width of 12.5mm, obtains the maximum resonant frequency of 6.7 GHz and minimal return loss -28dB. Similarly, slot L3 has better resonant frequency and return loss characteristics, which are nearly improved compared to the other slots.

3. Parametric Study

The primary objective of the parametric analysis is to investigate the return loss characteristics of the proposed antenna design's feed position, length of ground, and side effects.

In this case, the ground plane's size is essential in determining how well an enhanced impedance bandwidth may be achieved. In the work that has been proposed, the performance of the antenna has been significantly enhanced by optimising the ground length from 25 to 12.5 millimetres. This has led to an increased bandwidth, improved resonant frequency, and increased gain efficiency.

Table 2. The resonant frequency and return loss characteristics

Parameter	Length (mm)	Width (mm)	Resonant Frequency (GHz)	Return Loss (dB)
L1	12.5	12.5	6.7	-28
L3	8.5	0.5	6.6	-32
L4, L7	3.7	0.5	6.5	-33
L5, L8	3	0.5	6.5	-36
L6, L9	2.3	0.5	6.2	-48
L2	3.5	3.5	6.2	-48

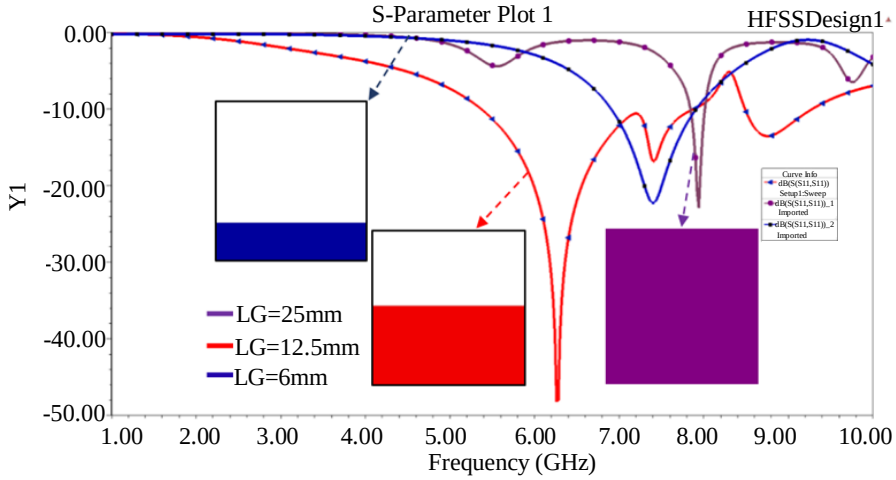

Fig. 4 Shows the influence of ground on return loss

Table 3. Comparative analysis among antennas having different ground lengths

Ground Length (mm)	Resonant Frequency (GHz)	Bandwidth	Return Loss (dB)
25	7.9	7.8-8 GHz 100 MHz	-22
12.5	7.4	6.9-7.9 GHz 1000 MHz	-22
6	6.2	5.3-7.8 GHz 2500 MHz	-48

As can be seen in Figure 4, the proposed model's predicted return loss characteristics are examined for ground lengths of Lg 25mm, 12.5mm, and 6mm. Additionally, the properties of the antennas with varying ground lengths are validated in Table 3, including the resonant frequency (in GHz), impedance bandwidth, and return loss (in dB). In the initial step of the modelling process, the ground is given dimensions of 25 millimetres in length and breadth.

This yields a resonance frequency of 7.9 gigahertz, a return loss of -22 decibels, and a narrowband width of 100 megahertz. As a direct result of this, the ground length has been reduced from 12.5mm to 6mm. In addition, the ground length was changed from 25 millimetres to six millimetres to acquire the best possible results. Based on the findings, the bandwidth of the antenna was significantly enhanced with only a small amount of return loss.

Moreover, the width of the feedline is modified to obtain a better impedance matching with a broader bandwidth, and the influence of the feed line on return loss is graphically presented in Figure 5. Here, the width of the feedline is considered to be 2.0mm, and the length of the feedline is 6mm. As shown in Table 4, it is identified that the antenna resonates from 5.8 GHz to 7.9 GHz and corresponds to the bandwidth from 0.36GHz to 2GHz, respectively. When the width of the feedline is reduced to 1mm, it resonates at 6GHz and 7.52GHz with bandwidths of 1.1 GHz and 0.2 GHz, respectively. In order to improve the impedance matching and bandwidth, the width is considered to be half of the length of the antenna (i.e., 3mm is considered as 2mm). Then, the width of the feed is taken as 1mm for the remaining half of the feed length; from the results, it is observed that there is good impedance matching and bandwidth efficiency with relatively low return loss.

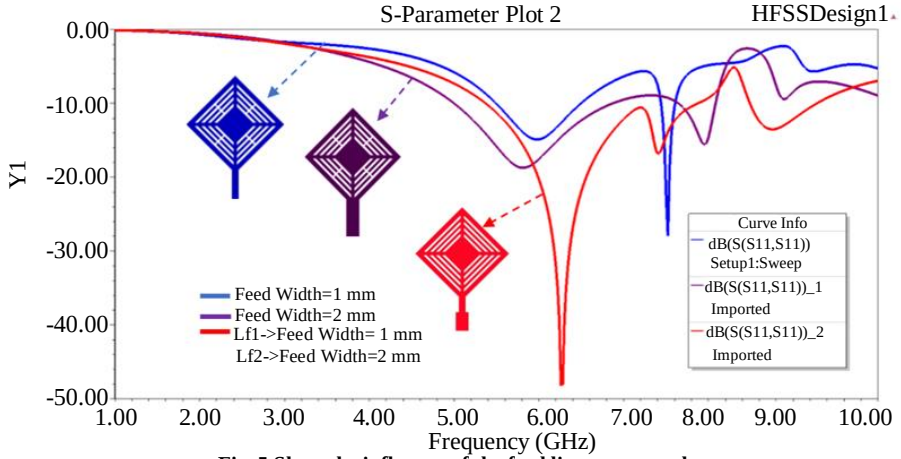

Fig. 5 Show the influence of the feed line on return loss

Table 4. Comparative analysis among antennas with different feed lengths and width

Feed Length (mm)	Feed Width (mm)	Resonant Frequency	Bandwidth	Return Loss (dB)
6	2	5.8 GHz	4.9 – 6.9 GHz 2000MHz	-18
6	1	6GHz	5.4-6.5 GHz 1100MHz	-14
The first half of feed length LF2 = 3	1	7.4GHz	7.7 – 7.15 GHz 550MHz	-16
The second half of feed length LF1 = 3	2	6.2GHz	5.3 – 7.8 GHz 2500MHz	-48

Using the Ansys HFSS tool, this study simulates the scattering parameter, radiation pattern, and efficiency of a solid diamond patch that does not have a fractal matching to 5.9 GHz. According to the findings, it can function at frequencies ranging from 5.6 GHz to 9 GHz, has a bandwidth of 3400 MHz, and exhibits a return loss of -28 dB at 6.7 GHz.

Furthermore, the T-shaped slots are loaded into the diamond patch at varying angles, such as 45°, 135°, 225° and 315° to improve the return loss at the desired frequency. Here, the S parameter chart is compared at varying iterations, such as 0^{th}, 1^{st}, 2^{nd}, 3^{rd}, and $4^{th,}$ as shown in Figure 6. In this work, the simulation of the antenna is performed concerning different iterations, and its iterative behaviour is analysed in terms of resonant frequency (GHz), bandwidth (MHz), and return loss (dB), as represented in Table 5. Figure 7 shows the quasi-static equivalent circuit model used to analyse the proposed DFFA's resonance frequency. This antenna design uses DFF rings with slits to provide a multiband tripe or double resonance frequency at 6.2 GHz. The DFFA has five rings: single DFF (N=1), double ring (N=2), N=3, N=4, and N=5. In the pass band, the Slot controls DFFA capacitance (CDFF) in the metal strip, and the metal strip controls DFF inductance (LDFF). The slit gap is crucial. DFFA resonance frequency is calculated using these models:

$$f_{DFFR} = \frac{1}{2\pi\sqrt{L_{DFFR}C_{DFFR}}} \quad (1)$$

$$C_{DFFR} = \frac{N-1}{2}[2L-(2N-1)(W+S)]C_0 \quad (2)$$

$$C_0 = \varepsilon_0 \frac{K\sqrt{1-K^2}}{K(k)} \text{ and } k = \frac{s/2}{w+s/2} \quad (3)$$

$$L_{DFFR} = 4\mu_0[L-(N-1)(S+W)]\left[ln\left(\frac{0.98}{\rho}\right)+1.84\rho\right] \quad (4)$$

$$\rho = \frac{(N-1)(W+S)}{1-(N-S)(W+S)} \quad (5)$$

Where N represents the number of DFF rings in the antenna, L denotes the average length of the CSRR, W denotes the width of the slot, which is 0.5mm, S signifies the spacing between the slots,

If N = 2, L = $\frac{L_4+W_4}{2}$ = 1.05mm

If N = 3, L = $\frac{L_5+W_5}{2}$ = 0.875mm

If N = 4, L = $\frac{L_6+W_6}{2}$ = 0.7mm

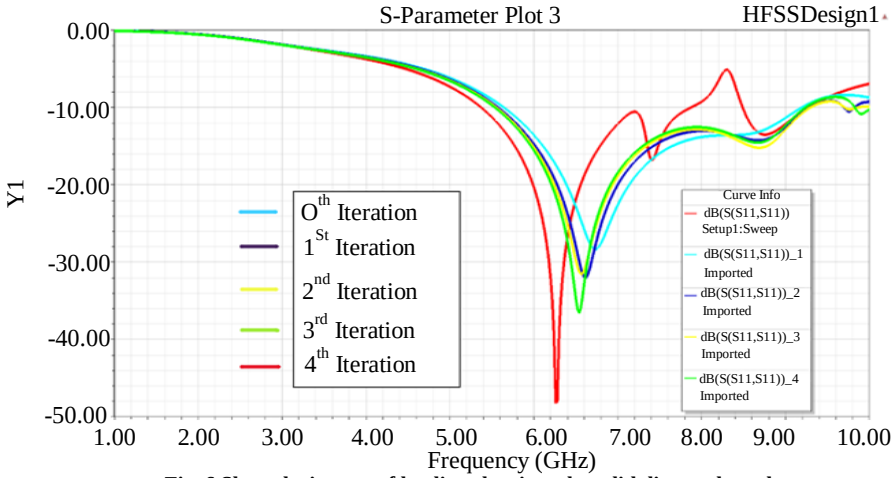

Fig. 6 Show the impact of loading slots into the solid diamond patch

Table 5. Performance analysis at different iterations of slot loading

Iteration	Resonant Frequency (GHz)	Bandwidth (MHz)	Return Loss (dB)
0^{th} iteration	6.7	3400	-28
1^{st} iteration	6.6	3800	-31
2^{nd} iteration	6.5	3800	-31
3^{rd} iteration	6.4	3700	-36
4^{th} iteration	6.2	2500	-48

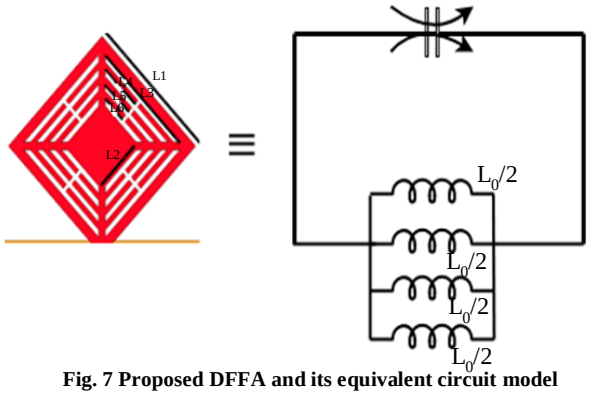

Fig. 7 Proposed DFFA and its equivalent circuit model

4. Results and Discussion

The suggested antenna's predicted and observed return loss are shown in Figures 8(a) and 8(b). This research found tripe band resonance at 6.3GHz, which is better for car applications. Then, the radiation pattern of the recommended antenna at 6.2GHz shows an omnidirectional H plane and a constant dipole E plane. Based on the feeder line and conducting substrate impedance mismatch, the Voltage Standing Wave Ratio is calculated. The lowest feasible VSWR value may be best for automobile application systems.

Figure 8 provides a visual representation of the far-field radiation pattern study that was carried out on the proposed antenna. In this particular instance, the results demonstrate that an omnidirectional pattern emerges in the plane of azimuthal projection.

However, an Elevation Plane (E-plane) projection reveals a pattern of a constant dipole. This is the case for all frequency bands (H-plane). The measure that is determined based on the impedance mismatching that exists between the feeder line and the conducting substrate is referred to as the Voltage Standing Wave Ratio (VSWR).

Figure 8 shows the Voltage Standing Wave Ratio (VSWR) of the proposed DFFA design concerning different frequencies (GHz). The fact that the Voltage Standing Wave Ratio (VSWR) achieves a perfect reduction in response to an increase in frequency from 2 GHz to 10 GHz, as determined by the results, is indicative of the superior performance of the suggested antenna design. The impedance chart of the suggested DFFA design can be shown in Figure 8. It is derived using the parameters of frequency, magnitude, angle, and other measurements. In most cases, the impedance plot is used to represent the value of the transmission line antenna's impedance in relation to the frequency.

In addition to this, it represents a number of different properties, such as impedance and admittance, as well as reflection coefficients. The Smith chart is generated for this evaluation in order to estimate the impedance of the DFFA in accordance with the Z & Y parameters and the reflection coefficients. As a consequence of the evaluation, it was determined that slot loading causes the resonance frequency to decrease and the input impedance to rotate clockwise. This results in an enhanced bandwidth and a shift in the location of the input impedance locus toward a lower impedance value.

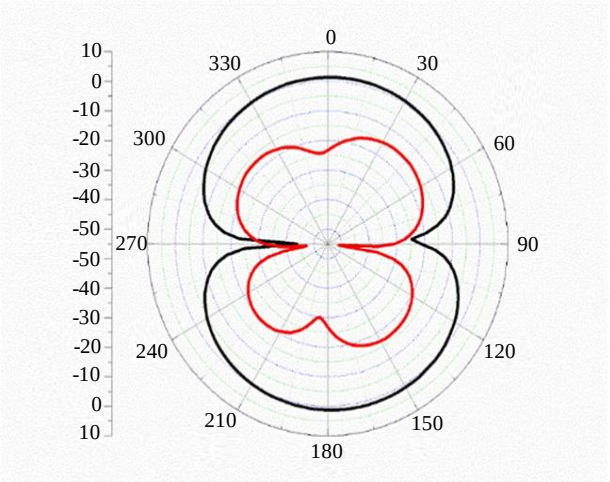

(a) E-Plane

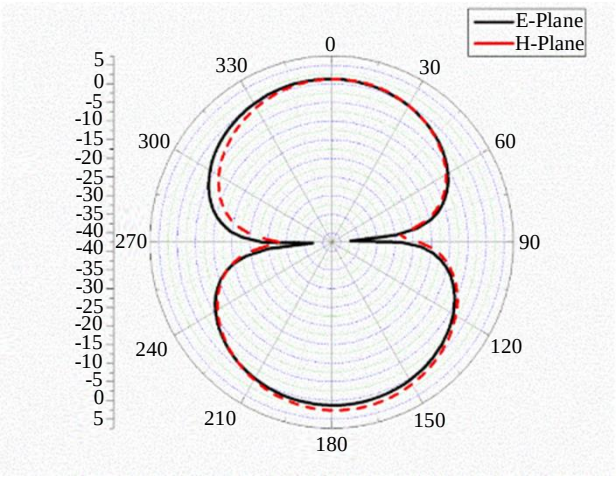

(b) H-Plane

Fig. 8 Simulated and measured far-field radiation patterns of the proposed antenna

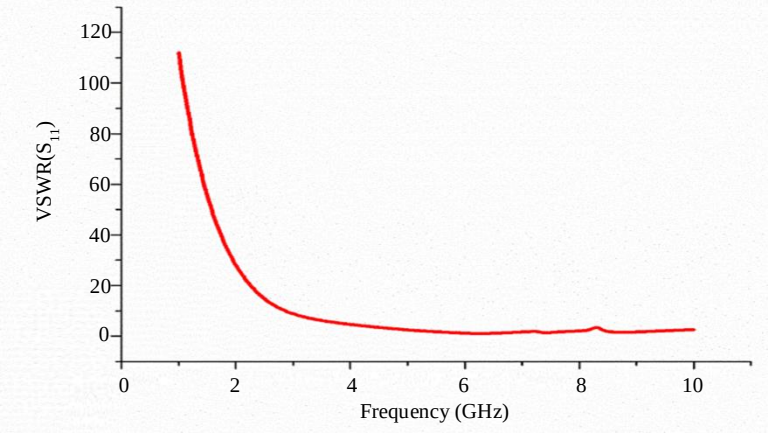

Fig. 9 VSWR analysis

Figure 9 presents the VSWR of the proposed DFFA design for varying frequencies in terms of (GHz). According to the results, it is analysed that the VSWR is ideally reduced with the increase of frequencies from 2GHz to 10GHz, which depicts the better performance of the proposed antenna design. The impedance chart for the suggested DFFA design may be seen in Figure 10, and it is based on the parameters of frequency, magnitude, angle, and other metrics.

In most cases, the impedance plot is used to represent the value of the transmission line antenna's impedance in relation to the frequency. In addition to this, it represents a number of other properties, such as impedance and admittance, as well as reflection coefficients.

For this assessment, a Smith chart is constructed to calculate the impedance of the DFFA in accordance with the Z&Y parameters and the reflection coefficients. From the evaluation, it is analysed that the resonance frequency decreased and input impedance rotates clockwise with slot-loading, which results in increased bandwidth and input impedance locus shift towards a lower impedance value. Table 6 gives the details of the comparison with different literature papers.

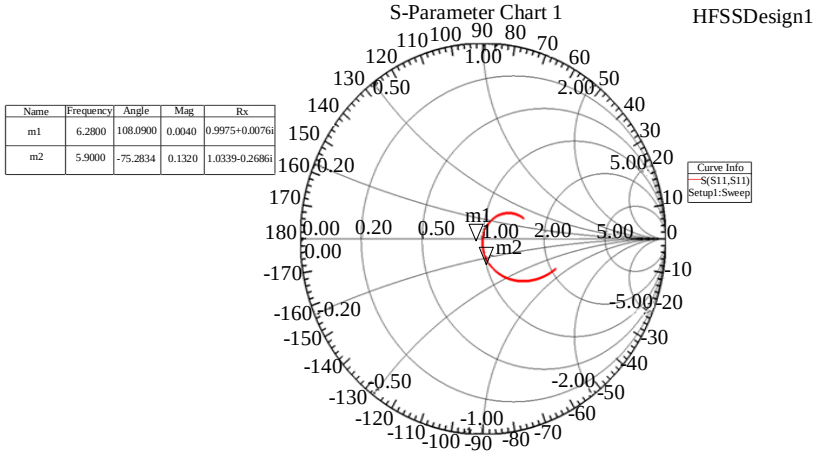

Fig. 10 S-parameter analysis

Table 6. Comparison table for antenna design with reference papers

References	Dimension	No. of Bands	Resonant Frequency GHz	Mathematical Property Verification
6	34*32	2	3.2,4.5	Not Verified
8	30*20	3	5.63	Not Verified
10	30*21	5	3.28 to 4.53	Not Verified
15	34*30	6	2.4,3.3	Not Verified
Proposed Work	25*25	Function with Many Frequency Bands	6.5	Verified

5. Conclusion

In this article, a novel DFFA with the dimensions 25 by 25 by 1.6 mm^3 is built specifically for use in automobile application systems. Additionally, the suggested antenna design has improved capabilities for functioning across many frequency bands. Then, the work presents its distorted omnidirectional radiation pattern, which is quite helpful for the application systems that are used in vehicles and environments with multiple paths.

According to the results of the simulation analysis, it is possible to use DFFA for V2X communications while using low-power transmitters. In addition to this, it achieved a gain efficiency improvement of 4.5 dB while maintaining a good radiation pattern. The suggested antenna has a greater beam width of 100 degrees and a response that is circularly polarised; as a result, it has the potential to be investigated for use in a variety of multi-standard wireless systems, including a vehicular application. It helps to improve both the quality factor and the impedance bandwidth when the partial ground plane is used. During the analysis, the DFFA will be built, and its radiation characteristics will be examined.

Additionally, the simulated results will be checked and compared with regard to the resonant frequency, impedance bandwidth, and return loss. The suggested antenna design has several advantages, the most important of which are its compact size, improved multiband properties, and compatibility with various vehicular communication systems. Increasing the number of iterations on this antenna design significantly improves both the bandwidth and the reflection coefficient.

With the help of previous discoveries and observations, it has been determined that a straightforward technique of a broadband antenna is doable by using a diamond-shaped patch of appropriate dimension. This has led to the conclusion that a suitable feed impedance matching may be achieved.

References

[1] Samson Daniel R., Pandeeswari R., and Raghavan S., "Offset-Fed Complementary Split Ring Resonators Loaded Monopole Antenna for Multi-Band Operations," *AEU-International Journal of Electronics and Communications*, vol. 78, pp. 72-78, 2017. [CrossRef] [Google Scholar] [Publisher Link]

[2] Tapas Mondal et al., "A Novel Tri-Band Hexagonal Microstrip Patch Antenna Using Modified Sierpinski Fractal for Vehicular Communication," *Progress in Electromagnetics Research C*, vol. 57, pp. 25-34, 2015. [CrossRef] [Google Scholar] [Publisher Link]

[3] Ioannis P. Gravas et al., "Optimal Fractal Antenna for In-Vehicle Entertainment Application," *2020 Wireless Telecommunications Symposium (WTS)*, Washington, DC, USA, pp. 1-5, 2020. [CrossRef] [Google Scholar] [Publisher Link]

[4] Minyeong Yoo, and Sungjoon Lim, "SRR and CSRR-Loaded Ultra-Wideband (UWB) Antenna with Tri-Band Notch Capability," *Journal of Electromagnetic Waves and Applications*, vol. 27, no. 17, pp. 2190-2197, 2013. [CrossRef] [Google Scholar] [Publisher Link]

[5] Amer T. Abed, Mahmood J. Abu-AlShaer, and Aqeel M. Jawad, *Fractal Antennas for Wireless Communications*, Modern Printed-Circuit Antennas, IntechOpen, pp. 1-27, 2020. [CrossRef] [Google Scholar] [Publisher Link]

[6] Mariem Aznabet et al., "A Coplanar Waveguide-Fed Printed Antenna with Complementary Split Ring Resonator for Wireless Communication Systems," *Waves in Random and Complex Media*, vol. 25, no. 1, pp. 43-51, 2015. [CrossRef] [Google Scholar] [Publisher Link]

[7] Rifaqat Hussain et al., "A Compact Sub-GHz Wide Tunable Antenna Design for IoT Applications," *Electronics*, vol. 11, no. 7, pp. 1-14, 2022. [CrossRef] [Google Scholar] [Publisher Link]

[8] R. Boopathi Rani, and S.K. Pandey, "ELC Metamaterial Based CPW-Fed Printed Dual-Band Antenna," *Microwave and Optical Technology Letters*, vol. 59, no. 2, pp. 304-307, 2017. [CrossRef] [Google Scholar] [Publisher Link]

[9] Abdul Rahim, Praveen Kumar Malik, and V.A. Sankar Ponnapalli, "Design and Analysis of Multi Band Fractal Antenna for 5G Vehicular Communication," *TEST Engineering & Management*, vol. 83, pp. 26487-26497, 2020. [Google Scholar] [Publisher Link]

[10] Tapas Mondal, Sanya Suman, and Shibu Singh, "Novel Design of Fern Fractal Based Triangular Patch Antenna," *2020 National Conference on Emerging Trends on Sustainable Technology and Engineering Applications (NCETSTEA)*, Durgapur, India, pp. 1-3, 2020. [CrossRef] [Google Scholar] [Publisher Link]

[11] Ravi Pratap Singh Kushwah et al., "A Novel Modified Hexagonal Fractal Antenna (HFA) with Band Notches for WLAN Rejection," *Journal of Electrical and Electronics Engineering Research*, vol. 11, no. 2, pp. 9-16, 2021. [CrossRef] [Google Scholar] [Publisher Link]

[12] Zsolt Szalay et al., "5G-Enabled Autonomous Driving Demonstration with a V2X Scenario-in-the-Loop Approach," *Sensors*, vol. 20, no. 24, pp. 1-24, 2020. [CrossRef] [Google Scholar] [Publisher Link]

[13] Salah Hamdy et al., "A New Fractal-Like Tree Structure of Circular Patch Antennas for UWB and 5G Multi-Band Applications," *2016 Progress in Electromagnetic Research Symposium (PIERS)*, Shanghai, China, pp. 2467-2467, 2016. [CrossRef] [Google Scholar] [Publisher Link]

[14] Raghavendra Karanam, and Deepti Kakkar, "Artificial Neural network Optimized Ultra Wide Band Fractal Antenna for Vehicular Communication Applications," *Transactions on Emerging Telecommunications Technologies*, vol. 33, no. 12, 2022. [CrossRef] [Google Scholar] [Publisher Link]

[15] Anirban Karmakar, "Fractal Antennas and Arrays: A Review and Recent Developments," *International Journal of Microwave and Wireless Technologies*, vol. 13, no. 2, pp. 173-197, 2021. [CrossRef] [Google Scholar] [Publisher Link]

[16] Narinder Sharma, and Sumeet Singh Bhatia, "Performance Enhancement of Nested Hexagonal Ring-Shaped Compact Multi-Band Integrated Wideband Fractal Antennas for Wireless Applications," *International Journal of RF and Microwave Computer-Aided Engineering*, vol. 30, no. 3, 2020. [CrossRef] [Google Scholar] [Publisher Link]

[17] Srivalli Gundala et al., "Compact High Gain Hexagonal Fractal Antenna for 5G Applications," *2019 IEEE International Conference on Advanced Networks and Telecommunications Systems (ANTS)*, Goa, India, pp. 1-7, 2019. [CrossRef] [Google Scholar] [Publisher Link]

[18] Arun Kumar Singh et al., "Design and Implementation of Microstrip Array Antenna for Intelligent Transportation Systems Application," *Frequenz*, vol. 75, no. 7-8, pp. 267-273, 2021. [CrossRef] [Google Scholar] [Publisher Link]

[19] Balaka Biswas, Rowdra Ghatak, and D.R. Poddar, "A Fern Fractal Leaf Inspired Wideband Antipodal Vivaldi Antenna for Microwave Imaging System," *IEEE Transactions on Antennas and Propagation*, vol. 65, no. 11, pp. 6126-6129, 2017. [CrossRef] [Google Scholar] [Publisher Link]

[20] Tharanga Premathilake et al., "High Directivity Broadband Hexagonal Fractal Ring Antenna with Modified Ground," *ECTI Transactions on Electrical Engineering, Electronics, and Communications*, vol. 18, no. 1, pp. 1-8, 2020. [CrossRef] [Google Scholar] [Publisher Link]